

DEPARTMENT OF ATMOSPHERIC SCIENCES

University of Washington

Semi-Annual Report  
on Contract NASA NsG-632

ON THE USES OF INTERMEDIATE INFRARED  
AND MICROWAVE INFRARED  
IN METEOROLOGICAL SATELLITES

by

Konrad J. K. Buettner

Robert Dana

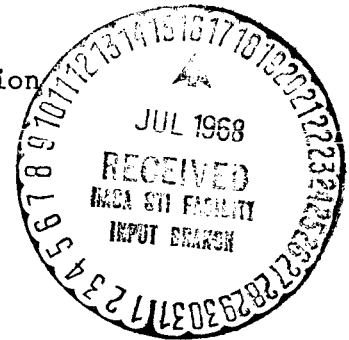
Kristina Katsaros

William Kreiss

Lee Martin

Prepared for

National Aeronautics and Space Administration  
Goddard Space Flight Center  
Greenbelt, Maryland



N 68-28922

(ACCESSION NUMBER)

(THRU)

(PAGES)

(CODE)


(NASA CR OR TMX OR AD NUMBER)

(CATEGORY)

FACILITY FORM 602

## FOREWORD

This semi-annual report deals with the activities in the fields of microwave evaluation of sea surface temperatures and of 10  $\mu$  emissivities. Included is a short paper submitted for publication to the Journal of Geophysical Research. A part of our activities is contained in the Doctoral Thesis of William Kreiss, entitled "Meteorological Observations with Passive Microwave Systems," also available as BSRL document D1 - 82 - 0692 from Boeing Scientific Research Laboratories in Seattle

  
Konrad J. K. Buettner

14 June 1968

Discussion of paper by S. F. Singer and G. F. Williams, Jr. "Microwave detection of precipitation over the surface of the ocean." Konrad J. K. Buettner, Department of Atmospheric Sciences, University of Washington, Seattle, Washington 98105 and William T. Kreiss, Boeing Scientific Research Laboratories, Seattle, Washington 98124.

Early analyses of microwave signals from a raining cloud [Buettner 1963, and Buettner in Kellogg, Buettner and May 1964] showed that rain emission could possibly be differentiated from ocean emission. Emissivity was determined from measured attenuation and its subdivision in absorption and scattering. This subdivision was based on Deirmendjian's [1960] use of a Mie - theory calculation. Since the ocean is highly reflective the multiple ray passes have to be taken into account, as shown in fig. 14 of Kellogg et al [1964]. It was also stated [Buettner 1963] that: "very dense non-raining clouds have similar, but smaller effect, whereas water in the form of ice, dust, haze, vapor and light clouds has little influence."

These latter estimates have been evaluated in detail by Kreiss [1968] calculating the absorption and emission by water vapor, and by water droplets of certain sizes; this calculation was made for "seeing" ground to sky, and satellite to ground, the ground being land or sea. These calculations show a definite effect of cloud droplets and water vapor down to frequencies of 15 GHz. The results were experimentally confirmed by a radiometer ground to sky in Seattle and one airplane to ocean from flight data of Catoe, Nordberg, Thaddeus and Ling [1967], all tests being made near 19 GHz.

It seems therefore justified to apply Kreiss' calculations to the airplane measurement of Singer and Williams [1968]. They find with a 15.8 GHz radiometer looking nadirwards, a brightness temperature for cloudfree ocean of 150°K and over a shower 200°K. This difference of 50°K could be rain, as Singer and Williams claim. But it is more likely a cloud of, e.g., 2384 m layer thickness and about  $1.0 \text{ gm m}^{-3}$  of liquid water content as shown in fig. 5.23 of Kreiss. From fig. 4 of Singer and Williams it appears that the effects of both rain and clouds are evident. The core of the shower could probably correspond to the highest temperatures of approximately 210°K, but it is noted

that the temperature at the end of the data run are about 15°K higher than those at the start. We believe that the clouds play an important role here and complicate the interpretation of the measured brightness temperatures in terms of rain rate without more supporting information.

References

- Buettner, K.J.K., Regenortung von Wettersatelliten mit Hilfe vom Zentimeterwellen (Rain localization from a weather satellite via centimeter waves), Naturwiss 50, 591, 1963.
- Catoe, C. W. Nordberg, P. Thaddeus, and G. Ling, Preliminary results from aircraft flight tests of an electrically scanning microwave radiometer, Tech. Rept. X - 662-67-352, Goddard Space Flight Center, Greenbelt, Maryland, 1967.
- Deirmendjian, D., "Atmospheric Extinction of Infra-Red Radiation," Quart. J. Roy. Meteor Soc., Vol. 86, 1960, pp. 371-381.
- Kellogg, W.W., K.J.K. Buettner and E.C. May, Meteorological Satellite Observations of Thermal Emission. RAND Corp. Mem. RM-4392-NASA, December 1964.
- Kreiss, W.T., Meteorological Observations with Passive Microwave Systems. Boeing Scientific Research Laboratories Document D1-82-0692, February 1968.
- Singer, S.F. and G. F. Williams, Microwave Detection of Precipitation Over the Surface of the Ocean. J. Geophys. Res., 73, 3324, 1968.

Submitted to the Journal of Geophysical Research 4 June 1968.

MICROWAVE REPORT

Progress in the microwave region of the spectrum has been concentrated in the application of the integrated equations of radiative transfer to the analysis of data from the NASA Convair 990 flights of May 5 through June 8, 1967. Work so far has been concerned with the over-water portions of the flight and with cloud-free atmospheres.

Assuming a horizontally stratified atmosphere, the transmissivity of the atmosphere decreases with increasing zenith angle because of the increase in path length according to the relationship  $\tau_a = \exp(-\alpha_0 \sec\phi)$  where  $\alpha_0$  is the vertical attenuation. Now for cloud-free conditions, we can neglect reflection, and the emissivity of the atmosphere is given by  $\epsilon_a = 1 - \tau_a$  or,  $\epsilon_a = 1 - \exp(-\alpha_0 \sec\phi)$

Now assuming a smooth specular reflecting surface, the emissivity for horizontal and vertical polarization can be written as

$$\begin{aligned}\epsilon_{||}(\phi) &= 1 - |R_{||}(\phi)|^2 \\ \epsilon_{\perp}(\phi) &= 1 - |R_{\perp}(\phi)|^2\end{aligned}$$

where  $R_{||}(\phi)$  and  $R_{\perp}(\phi)$  are the Fresnel reflection coefficients for horizontal and vertical polarization respectively at the incident angle and are given by (Kerr, 1965)

$$\begin{aligned}R_{||}(\phi) &= \frac{\cos\phi - \sqrt{e - \sin^2\phi}}{\cos\phi + \sqrt{e - \sin^2\phi}} \\ R_{\perp}(\phi) &= \frac{e \cos\phi - \sqrt{e - \sin^2\phi}}{e \cos\phi + \sqrt{e - \sin^2\phi}}\end{aligned}$$

In these equations  $e$  is the relative dielectric constant of the water and has the value of 59 for sea water in this region of the spectrum. Graphs of the emissivity and reflectivity for both horizontal and vertical polarizations are given in Figures 1 and 2.

Neglecting the effects of solar radiation, the brightness temperature as seen by the downward viewing radiometer is given by the following expression, where  $\epsilon_w(\phi)$  and  $r_w(\phi)$  are the values for horizontally polarized radiation, since the radiometer was only responsive to this radiation.

$$T_b = \epsilon_w(\phi) T_w \tau_a + r_w(\phi) \epsilon_a T_m \tau_a + \epsilon_a T_m$$

The first term is the contribution from the water surface, the second term is the radiation emitted by the atmosphere and reflected by the water and the third term is the contribution from the atmosphere between the water surface and the radiometer. A graph of theoretical brightness temperatures versus incident angle for various values of vertical transmissivity and for a smooth water surface is given in Figure 3.

The effect of a rough surface is to distribute the reflected or emitted energy away from the nadir angle; the rougher the surface the greater is the effect. One method of determining an effective emissivity is to assume specular reflection and then integrate the angular distribution of emissivity for a smooth surface over the distribution of slopes of the water surface. Using slope distributions given by Cox and Munk (1954), rough calculations have been made using this method and the effect is to increase the emissivity at large angles of incidence. A schematic diagram of the effect is given in Figure 4, for increasing values of sea roughness. A computer program to provide quantitative values for the emissivity is currently being worked on.

A theoretical study of the effect of various sea states on the brightness temperatures seen with a downward viewing radiometer has been calculated by F.J. Janza of Ryan Electronics and Space Systems (1968), and his results are shown in Figure 5. The net effect is to increase the temperatures seen at large viewing angles, until for very rough seas, the radiometer sees almost a constant brightness temperature for the range of viewing angles.

The curves shown in Figure 5 would be the average values that would be observed, actual data should show variations from point to point, depending on the actual amount of specular reflection at each instant. A typical curve showing one complete scan off the coast of California

and for cloudless sky conditions is shown in Figure 6.

One effect which has been left out of the development so far has been the influence of solar radiation. In the spectral range of interest, the sun emits like a black body at 6000 K. Thus for a smooth surface and the radiometer looking at the sun's image on the water surface, the increase in brightness temperature due to the sun would be given by the following equation,

$$T_b = (3 \times 10^3 \text{ }^\circ\text{K}) r_w(\phi) \tau_a^2 r_s \cdot r_b^2$$

where:  $r_w(\phi)$  = the reflectivity of the water

$\tau_a$  = the transmissivity of the atmosphere

$r_s$  = the radius of the solar image in degrees

$r_b$  = the radius of the antenna beam in degrees

and the temperature of the sun has been reduced by one-half because of the polarization of the radiometer. Therefore, using the sun's diameter as 0.5 degrees and the beam diameter as 2.7 degrees, and a vertical transmissivity of 0.9, the effect of solar radiation would increase the brightness temperature by 50°K if the sun was directly overhead.

For a rough surface, the solar radiation would be reflected over a variety of angles, decreasing the temperature from the maximum seen with a smooth surface. To calculate the magnitudes for a rough surface, an integration of the solar intensity over the distribution of slopes and in the direction of the antenna would have to be done. Rough estimates have been made using this technique and increases of 10°K to 20°K would be expected. A computer program to obtain more accurate results is being planned at this time.

Evidence that these values are reasonable can be seen in Figures 7 and 8. Figure 7 shows the brightness temperatures off the California coast seen at nadir viewing angles and with a cloudless atmosphere.\* The large variations could be due to the specular reflection of solar radiation. Figure 8 shows two scans taken over the North Pacific Ocean approximately six minutes apart. The only difference between the two curves is that the aircraft changed course by 50 degrees and hence its direction of scan in relation to the sun. Thus it appears that the sun has an effect which must be taken into account before

\* during Nasa Convair flight.

any quantitative values of the brightness temperatures can be obtained.

Once the effects of sea roughness on the effective emissivity and the solar radiation are determined, then the real analysis of the data can begin. That is determining the water vapor content of the atmosphere from the angular distribution of brightness temperature and determining the effect of clouds in the radiation field.

#### FUTURE WORK

1. Determination of effective ocean emissivities for various values of surface roughness. Theoretical values can be determined by the method outlined above and then compared with the data, where values of surface roughness could be determined from the aerial photographs.

2. More work is needed on the influence of solar radiation. Using a computer program, theoretical values of the angular distribution of the solar increase of temperatures for various elevation angles and directions of scan can be determined and then compared with the observed data.

3. Once the effective emissivity and influence of solar radiation are given quantitative values, the determination of water vapor content of the atmosphere using the angular distribution of brightness can be worked on. Verification could be obtained by comparing the synoptic data closest to flight times and track.

4. Another major area of study would be the influence of clouds in the radiation field. Employing various models used in Bill Kreiss's thesis (1968), the effect of clouds on the surface brightness temperatures can be determined.

5. Further analysis of the data over other portions of the flight can be analysed. Included in this would be comparison of fresh water lakes to that of sea water, emission over ice fields and snow fields and their variation with angle and variations over various types of land features.



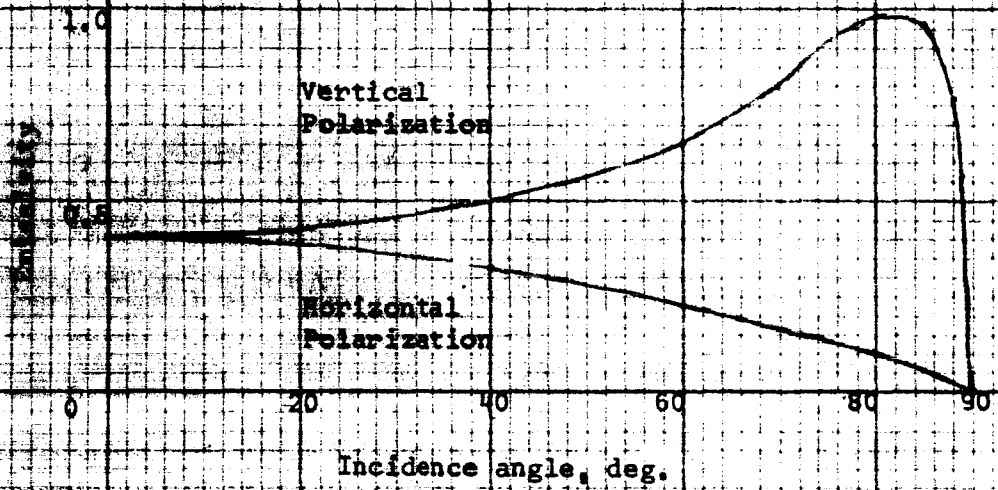


Fig. 1. Variation of emissivity with viewing angle for two polarizations

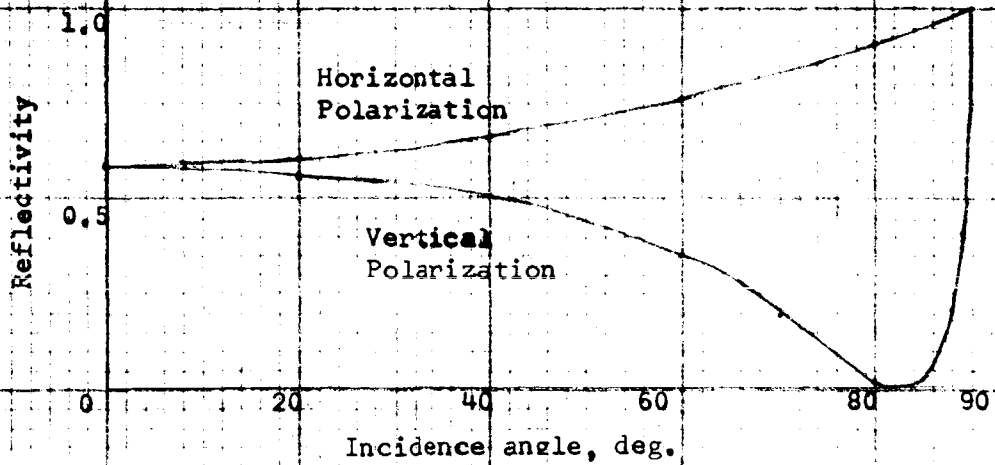


Fig. 2. Variation of reflectivity with viewing angle for two polarizations

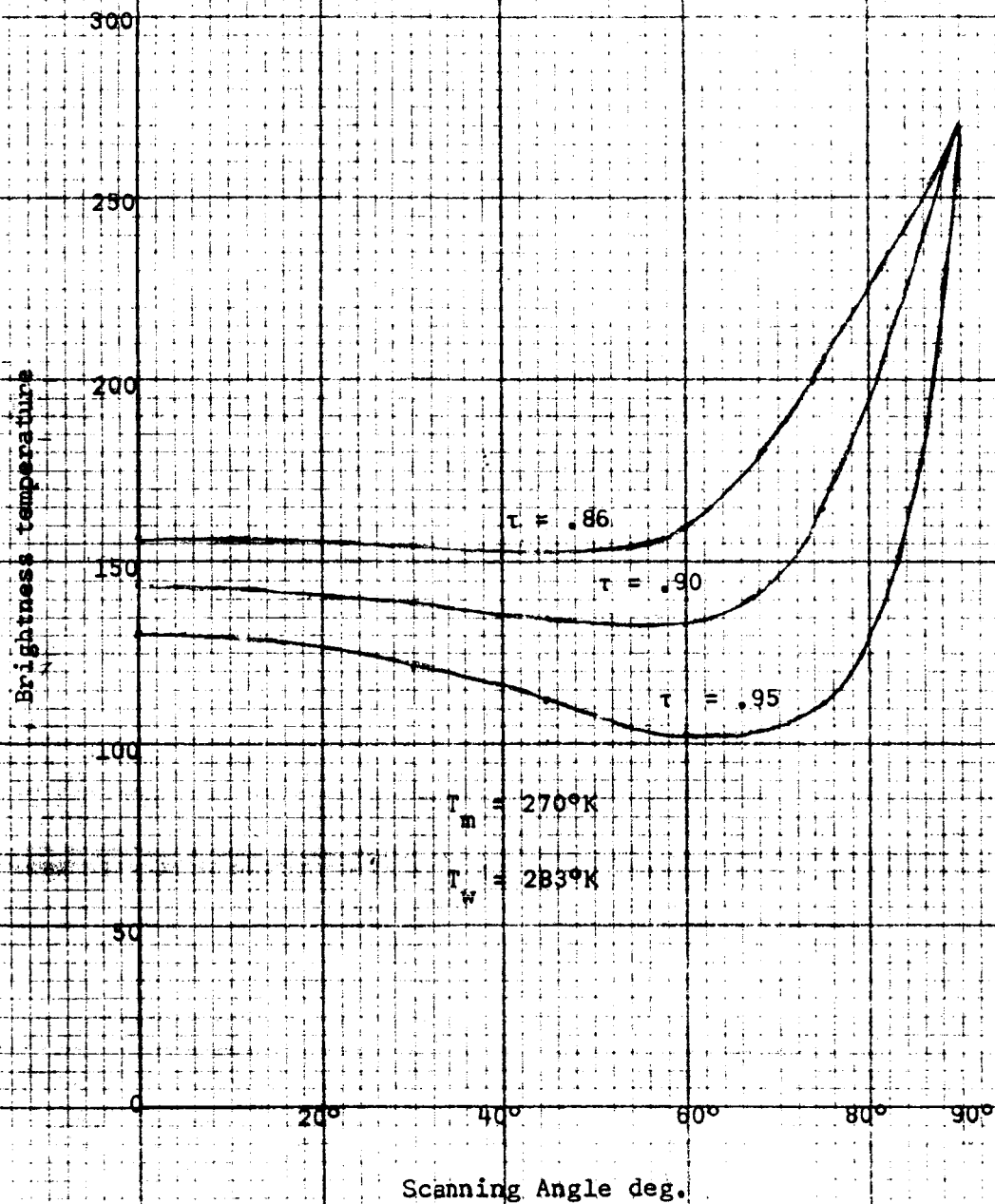


Fig. 3, Brightness temperature vs. scanning angle for various values of vertical transmissivity

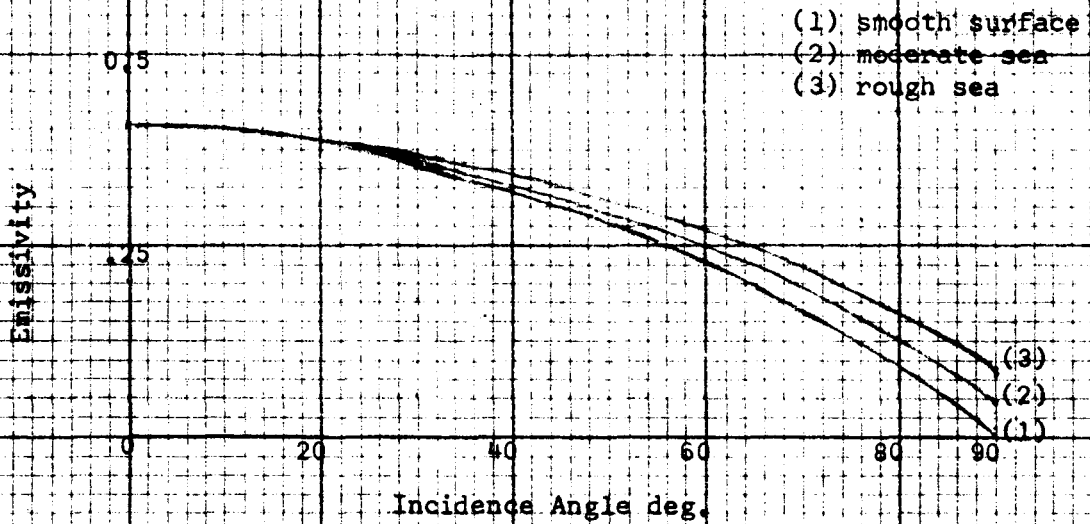


Fig. 4 Increase in Emissivity due to increasing sea roughness

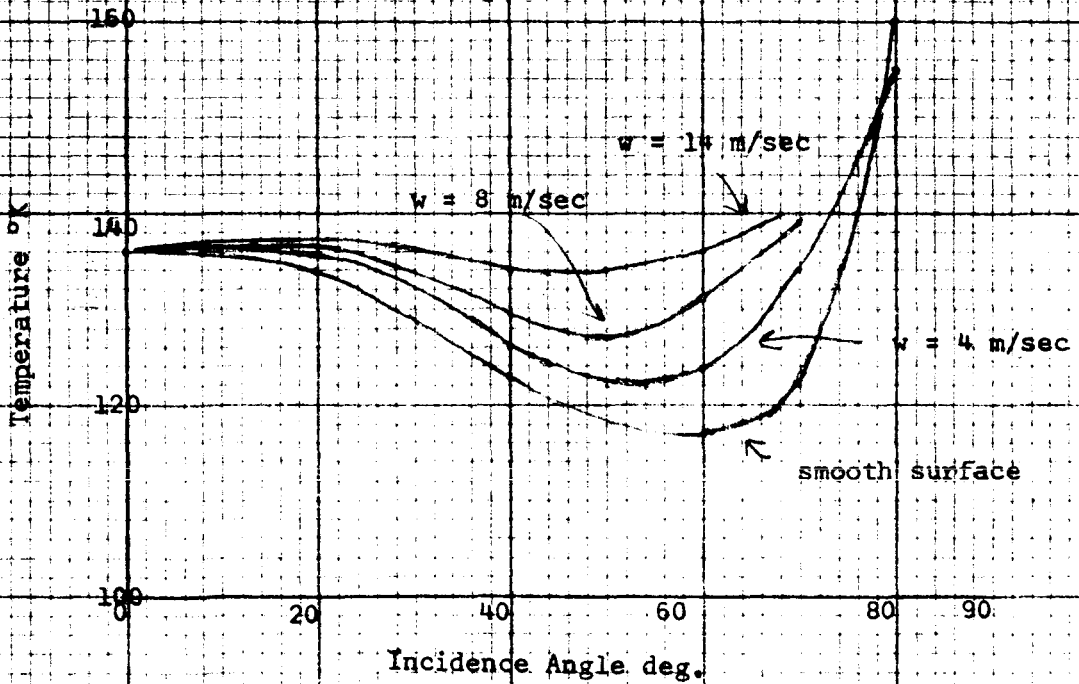


Fig. 5 Theoretical brightness temperatures for various wind speeds for a true surface temperature of 290°K (from Janza, 1967)

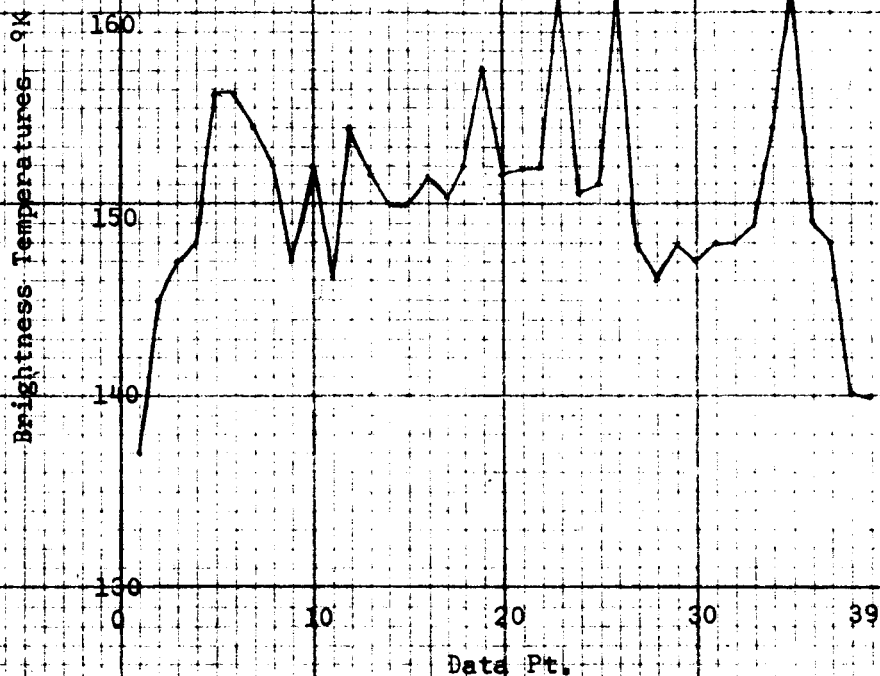


Fig. 6 Distribution of brightness temperature for Flt. #6, 20/45/00

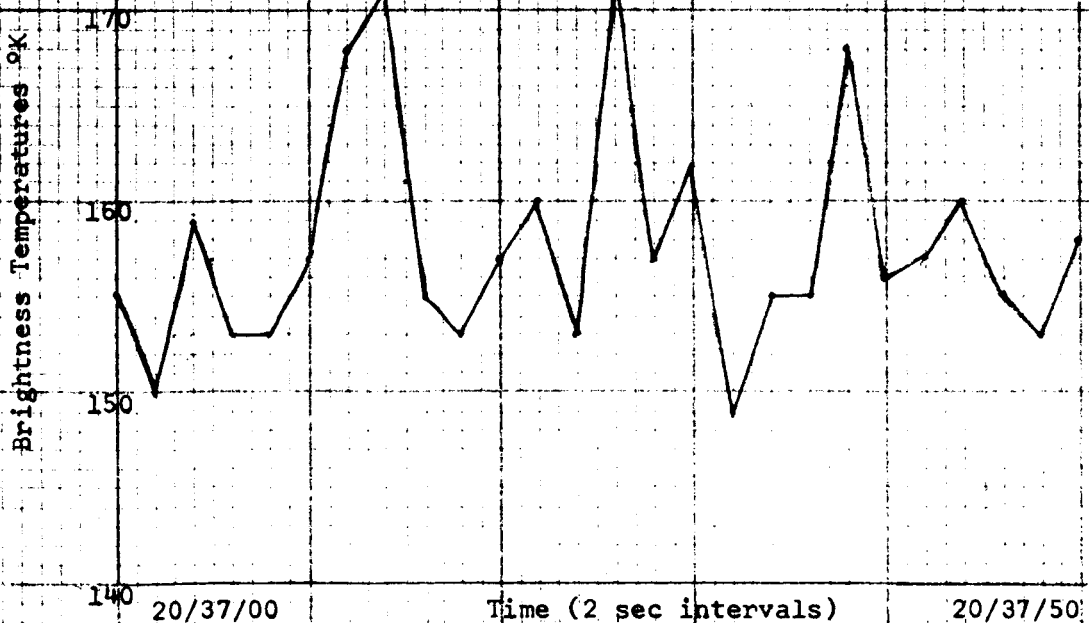
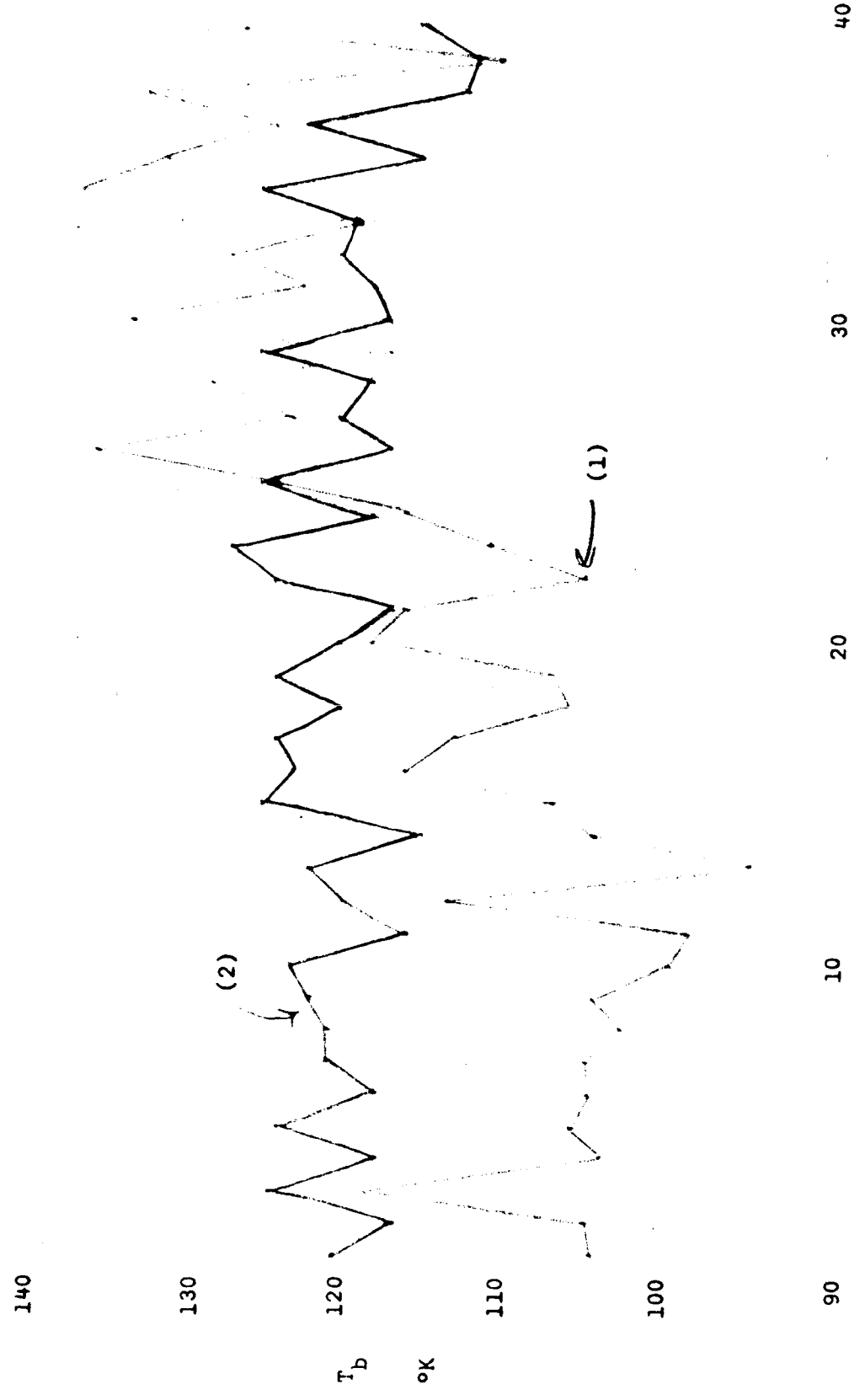


Fig. 7 Nadir brightness temperatures for Flt. #6, 149/20/37/00 to 149/20/37/50

Fig. 8 Two scans of brightness temperature over the North Pacific Ocean taken six minutes apart

- (1) curve (1) Time 150/00/26/04 scanning into solar image
- (2) curve (2) Time 150/00/20/00 scanning away from solar image



Data Pt.

## Sea Surface Report

### 1. Progress of the Study of the Influence of Rain on Sea Surface Temperature and Salinity.

During the past six months the main emphasis has been on experimental work. In the Third Annual Report on this contract (Buettner et al. 1967) the experimental set-up is described.

The salt water tank was placed out-of-doors during natural rainfall on several occasions, and the temperature and salinity profiles before, during and after the rain were observed. The details of the experiments will be given in a final report soon to appear, but a few generalizations can be made here. The frequency of large drops, which can be correlated with the rain rate, (See for instance Best (1950) or Blanchard (1953).) determines the depth to which the change in temperature and salinity will be observable. Laboratory experiments with monodisperse drop size distributions have also brought out that the larger drops are much more effective in producing mixing. This is consistent with the observations that a rain consisting of small drops produces the larger change in surface values for the same rain rate.\*

The experiments also show that the rain produced stability has pronounced effects on the heat and mass transport near the surface. Before the rain any surface cooling leads to convection and the temperature of the tank remains uniform throughout, except for a cool surface film, observable with the Barnes radiometer. After a rainfall the stable layer acts as a protective lid against mixing. There is now a deep layer in which all transfer of heat or mass is molecular. The surface layer can be cooling as well as warming without convection taking place, because the salinity gradient is much more than the temperature gradient, which determines the vertical gradient of density; since molecular transfer of heat is much larger than that of salt the temperature profile adjusts to the environmental influences in a matter of hours, while the salinity gradient remains almost unchanged for days after the rain has stopped. The salinity gradient is slowly

---

\* Figure 9 demonstrates these observations.

attributed by evaporation from the surface as the main cause rather than by salt-water diffusion.

### 3. Surface Reflectivity in the Visible as a Function of Temperature and Salinity.

In the Third Annual Report we discussed a very intriguing photogrammetric picture obtained with three visible and one near infrared filter, which supposedly displayed a difference between a salt water and a recently rained on area. The effect of dilution on reflectivity has since been calculated with the use of data on the refractive index of seawater of various salinities given for  $\lambda = 587.6 \mu$  by Defant (1961), and the Fresnel formula. The formula is greatly simplified by the fact that the index of absorption is negligibly small here, and reduces to the following form:

$$R = \frac{a^2 - 2a \cos\phi + \cos^2\phi}{a^2 + 2a \cos\phi + \cos^2\phi} = \frac{a^2 + \sin^2\phi \tan^2\phi}{a^2 + 2a \sin\phi \tan\phi + \sin^2\phi \cos^2\phi}$$

where  $n$  is index of refraction,  $\phi$  angle of incidence and  $a$  is defined through

$$a^2 = n^2 - \sin^2\phi$$

Data on  $(n - n_0)$  by Lubben (1913) given in Timmermans Tables (1956 - 1960), where  $n$  is the refractive index of a salt solution and  $n_0$  is that of pure water, show this quantity to be almost constant throughout the visible spectrum. Therefore our calculation should apply at least for the three filter regions in the visible. It is not known to the author, if there may be any drastic changes in the progression of the indices of refraction and absorption, when we enter the near infrared. Table I gives values of reflectivity for selected incidence angles and for several combinations of temperature and salinity. We see that the effect of salt concentration and temperature is exceedingly small, but increases somewhat with angle. Yost and Wenderoth claim

that their color-addition technique is capable of differentiating 7,500,000 color differences, as compared to 200 shades of gray, for the more conventional black and white photogrammetric methods. Their article does not describe any details of the particular rain shower that their photogrammetric picture detected. It would be of great interest to know the duration and intensity of the shower, and the time elapsed between the end of the rain and the time of the photograph. If the small change in reflectivity between say a 35 parts per thousand, 20°C saltwater surface and a 20 parts per thousand, 10 °C rain area, is really observable, their technique would be most powerful, and should have many applications in oceanography and meteorology.

There may, however, have been contributing circumstances here. The heavy rains of hurricane Inez, with which this rainfall was connected, may have produced runoff through storm sewers, which could be turbid water. Accompanying the rain may be other surface effects such as a temporary destruction of the naturally occurring thin oil film, and also, a difference in slope distribution of the sea surface, because of the impinging rain drops. There may remain a difference in the subsurface turbulence due to the stabilizing density stratification in the rain area, which may also affect the surface patterns. The effect on the reflective properties of the surface due to these possibilities has not been assessed.

### 3. A Proposal for Future Work.

As a follow up of the rain study, but with a broader view, it is proposed that the investigation of sea surface temperatures be continued by employing satellite radiometer data of the highest resolution available.

The effects on sea surface temperature of a passing hurricane have been reported from observations at coastal stations and a weather ship (Hazelworth, 1968), and by radiometric measurements from aircraft, (McFadden, 1968). The temperature change is in the order of 3 °C, and it takes 10 - 13 days for the surface temperature to return to normal. This local anomaly in the sea surface temperature should be observable in the more accurate satellite data. It is caused by a combination of



advection, upwelling, evaporation and rain cooling, and sensible and radiative heat losses at the surface. By use of satellite data the sea surface temperature could be related to the intensity and horizontal extension of the storm, the storm track, etc.

It may be possible with the ITOS HRIR (High Resolution Infrared Radiometer), but more likely by the VHRR (Very High Resolution Radiometer) described by Bandeen (1968), to observe the effects on sea surface temperature from the occurrence of a thunderstorm over an area such as the Gulf of Mexico. T.V. camera pictures, or photometric measurements in the visible, such as the visible channel of the MRIR (Medium Resolution Infrared Radiometer) collects, should be used together with the infrared radiation data. Preferably the visible and infrared data should be synchronous and geographically aligned, in order that low clouds and fog can be separated from warm ocean areas.

Since our group is not large, and this project would largely be the effort of one individual, it is proposed that detailed study be made of a few, well chosen cases only, but with as much supporting information as possible on meteorological and oceanographic conditions.

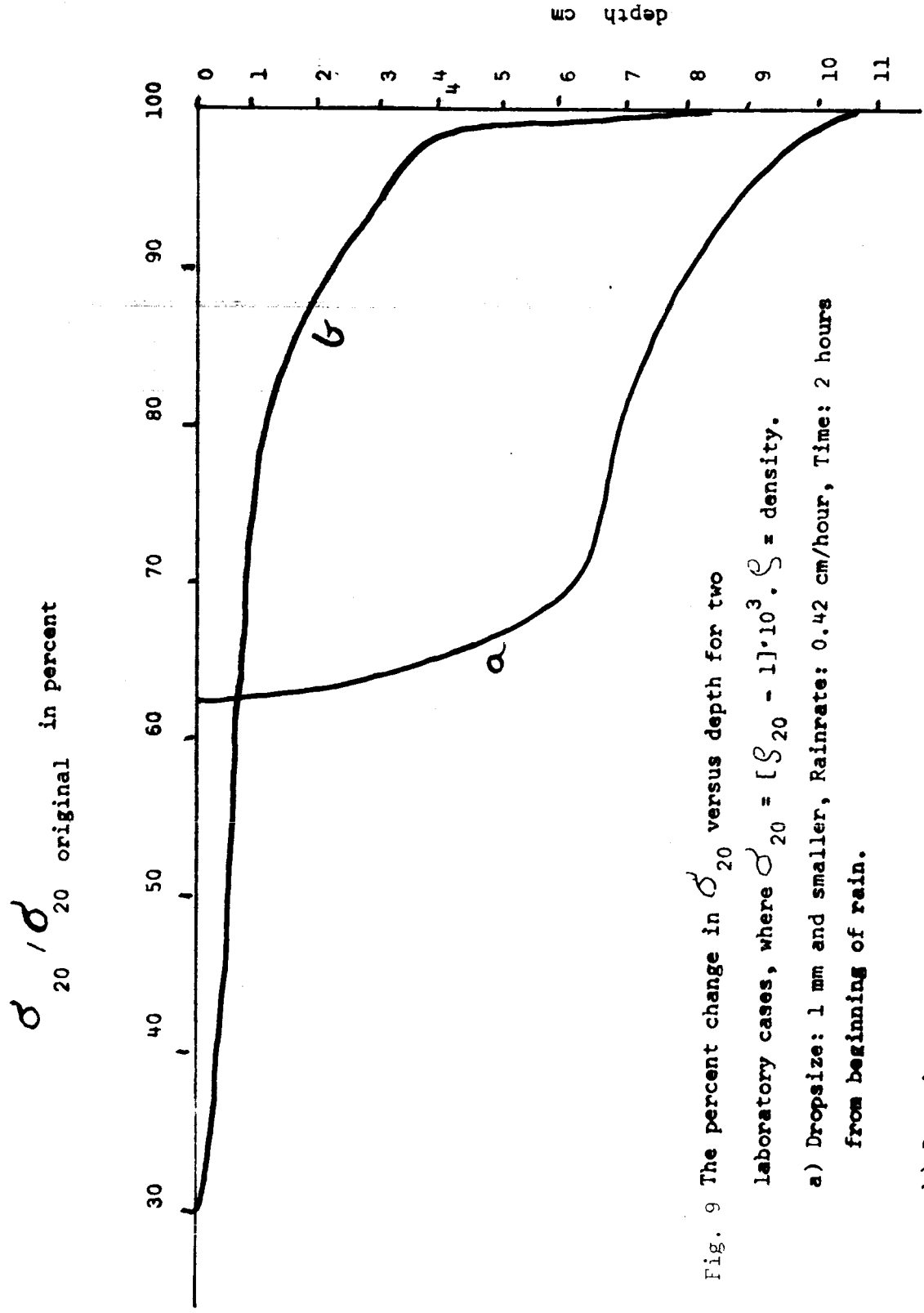


Fig. 9 The percent change in  $\sigma_{20}$  versus depth for two laboratory cases, where  $\sigma_{20} = [S_{20} - 1] \cdot 10^3$ .  $S$  = density.

a) Dropsize: 1 mm and smaller, Rainrate: 0.42 cm/hour, Time: 2 hours from beginning of rain.

b) Dropsize: 2.7 mm, Rainrate: 1.3 cm/hour, Time: 1 hour 10 min. from beginning of rain.

REFLECTIVITY OF SEA-WATER AS A FUNCTION OF  
SALINITY, TEMPERATURE, AND ANGLE FROM THE VERTICAL

$\lambda$	S <sup>o</sup> /∞∞	T <sup>o</sup> C	n	k	Angle from the vertical	R%
587.6	35	20	1.339801	.510 <sup>-8</sup>	0	2.109
					30	2.218
					45	2.87
					60	6.180
					80	35.014
	0	15	1.333338		0	2.041
					30	2.147
					45	2.794
					60	6.059
					80	34.803
	35	10	1.339995		30	2.185
					80	35.020
	20	10	1.337152		30	2.220
					80	34.928

### Infrared Emissivity Experiment

The results of measurements of a few sands and soils as shown in the Third Annual Report of this contract show a considerable decrease in 8 - 14 micron average emissivity at large viewing angles. The values are down 5 to 7 per cent at a 60 degree angle from the normal to the target surface. Subsequent data on solid and granulated minerals show the same effect. In order to determine if the angular dependence is truly that strong it was necessary to reconsider possible systematic errors.

An extensive check on the uniformity of temperature across the specimen surface was carried out by monitoring the temperature at various points with tiny thermocouples. Lead wires were laid across the top of the target material and up through the material, and in both cases no deviations in temperature from the value at the center were found greater than 0.25°C.

The field of view (FOV) of PRT-5 Barnes Infrared Thermometer is advertised as being "2° nominal". The design of the experiment allowed for twice that FOV, so that even at a viewing angle of 60° the target surface exceeded the viewable area. But recently it was necessary to undertake a measurement of the FOV for short object distances to see if the instrument was actually "seeing" outside the target area.

The infrared thermometer was set up to view normally through a hole in a blackened board to a plate painted black about 26 cm from the outer optical element. The center of the area being viewed was determined by positioning a flat circular aluminum mirror about 1.5 cm. in diameter on the black plate until a maximum output was acquired. This meant that infrared radiation from the 55°C detector cavity reflecting back to itself was a maximum; therefore the mirror was centered on the optical axis.

A hot black bead connected by a polished copper wire to a soldering iron was probed radially inward just above the background plane. It was verified that the image viewed by the PRT-5 is circular because points of equal signal enhancement for a constant background temperature

formed a circle.

The hot bead 4.0 mm in diameter was passed across the field of the PRT-5 and the positions noted using marks scaled off on the black plate. Fig. 10 shows the increase in radiance  $N$  versus the distance from the center divided by the increase for the bead at the center,  $\rho = 0$ . The angle  $\alpha$  is zero at the point directly under the edge of the aperture, which is 0.50 cm. in radius, and is equal to half the FOV as defined by marketing firms. It can be seen that the half-power point is at about  $\alpha = 1.2^\circ$  or an FOV of  $2.4^\circ$ , but the infrared thermometer actually views as far out as  $8^\circ$  on each side of center.

In fig. 11 the relative enhancement of radiance due to a ring of width equal to the bead width and of mean radius  $\rho$  is plotted. The values of fig. 10 were multiplied by the ratio of ring area to bead area, which is  $4\rho/a$ , where  $a$  is the bead radius. At  $\rho = 0$ , however, the proper ratio is  $\pi a^2/\pi a^2 = 1$ .

It can be concluded that for viewing a flat surface close to the PRT-5 the ring of maximum signal is about 0.5 degrees outside the projection of the instrument's aperture and the half power points is at about 3.5 degrees. A crude integration of the curve for fig. 11 reveals that half of the radiant power hitting the detector cell comes from  $\alpha$  greater than 1.9 degrees.

If the optical system of the PRT-5 is similar to an earlier model of Barnes instrument we have at the University of Washington, the PRT-4, it consists of a positive meniscus objective and a hyperimposed thermistor bolometer separated by three baffles and a filter, all in a temperature controlled cavity. The presence of the lenses means that this measurement of field of view at short object distances is probably not applicable to large object distances. The shape of plots like fig. 10 and fig. 11 would probably be different for a distant field.

A correction for this larger-than-expected field of view can be made from the results of this measurement in analyzing the existing emissivity data. Future angular measurements will be taken concurrently with angular views of a relatively good blackbody in the plane of the specimen surface.

Because of space limitation inside the cold box the inside reference blackbody is a thin, flat, aluminum plate painted with Parson's Optical Black laquer. The infrared emissivity of this paint was advertised as .98 based on the same value obtained by MacDowall (see annals of IGY v. 5) of the total emissivity for Parson's Black at 25°C. Ramsey (1964) reported that this paint applied to an aluminum substrate had an average specular reflectance, measured at a 30° angle of incidence, less than 0.5% for the wave length range 2.5 - 4.0 $\mu$ . Another very black paint according to this report was 3M Velvet Black Paint.

Conaway and Van Bavel (1966) obtained a value of .98 within 1.5% for Parson's Black sprayed over Parson's Primer. Values used by our research group, based on emissivity box measurements are .985 and .988.

I have measured the emissivity of Parson's Black paint by the method used by Conaway and Van Bavel (1966, 1967). The surface temperature of an aluminum plate painted with the primer and outer coating was varied over a range of about 10°C centered on a value of 26.9°C, and the vertical radiance was carefully recorded. The target was enclosed in the insulated, temperature controlled assembly inside the cold box, which was kept at approximately -70°C. The Parson's paint surface was intermittently exposed to view by the Barnes PRT-5 when its temperature was determined by thermocouples and known to be steady in time.

The temperature of the environment of the surface under scrutiny was kept constant, so that any change in the radiance as seen by the infrared thermometer was due to the term  $\bar{\epsilon}B(T)$ , where  $\bar{\epsilon}$  is the emissivity averaged over wave length and temperature and  $B(T)$  is the blackbody radiance integrated over the filter response of the infrared thermometer. The average emissivity is then a slope of the plot of effective blackbody radiance  $N$  for the temperatures given by the IR thermometer (carefully calibrated with a blackbody cavity of high quality) versus the effective blackbody radiance for the temperatures given by the thermocouples. The results are shown in fig. 12 and the value for  $\epsilon$  was  $.982 \pm .008$ .

Two copper-constantan thermocouples were mounted on the painted surface, having Teflon insulated wires painted with Parson's paint.

One was situated near the center and one near the edge to check for lateral nonuniformity in temperature. The centrally located thermocouple, 0.025 mm. in thickness, was mounted within 0.1 mm. of the surface with its tip apparently touching the paint.

A 1 mm. diameter hole was drilled from the center of the unpainted side of the aluminum plate almost through to the other side, leaving a microscopic opening in the painted surface. A thermocouple bead about 0.025 cm in size was then threaded into the hole and fitted into the hole's conical tip. The bead had been previously coated with Parson's primer. The surface to be measured was then given a fresh coat of the Optical Black laquer. This left the lower thermocouple in good thermal contact with the paint and with the topmost layer of the aluminum substrate.

When the upper and lower thermocouples were at the same temperature, vertical gradients in the paint were eliminated and measurements were taken.

Due to the shortage of supply of Parson's paint, I was forced to apply it by fine, soft brush rather than by spraying. Some coatings have yielded lower values of  $\bar{\epsilon}$ , but the high value can be obtained by brushing if the paint is adequately stirred or shaken.

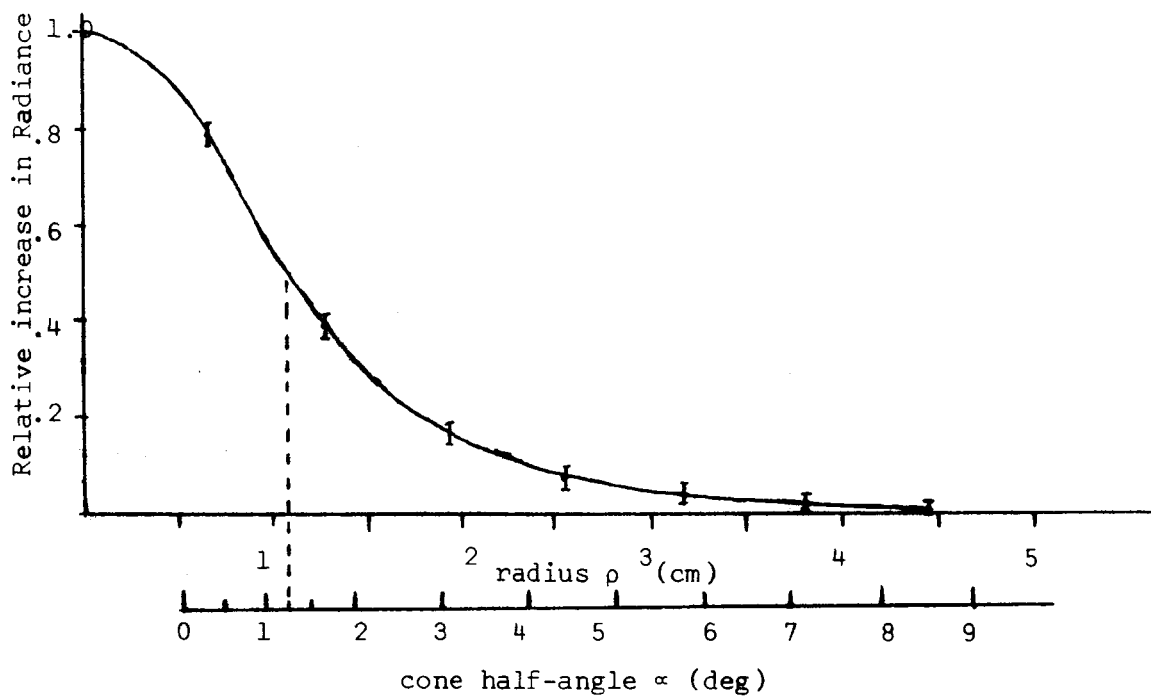


Fig. 10 Relative increase in radiance versus radial distance of hot bead from the optical axis at an object distance of 26 cm.

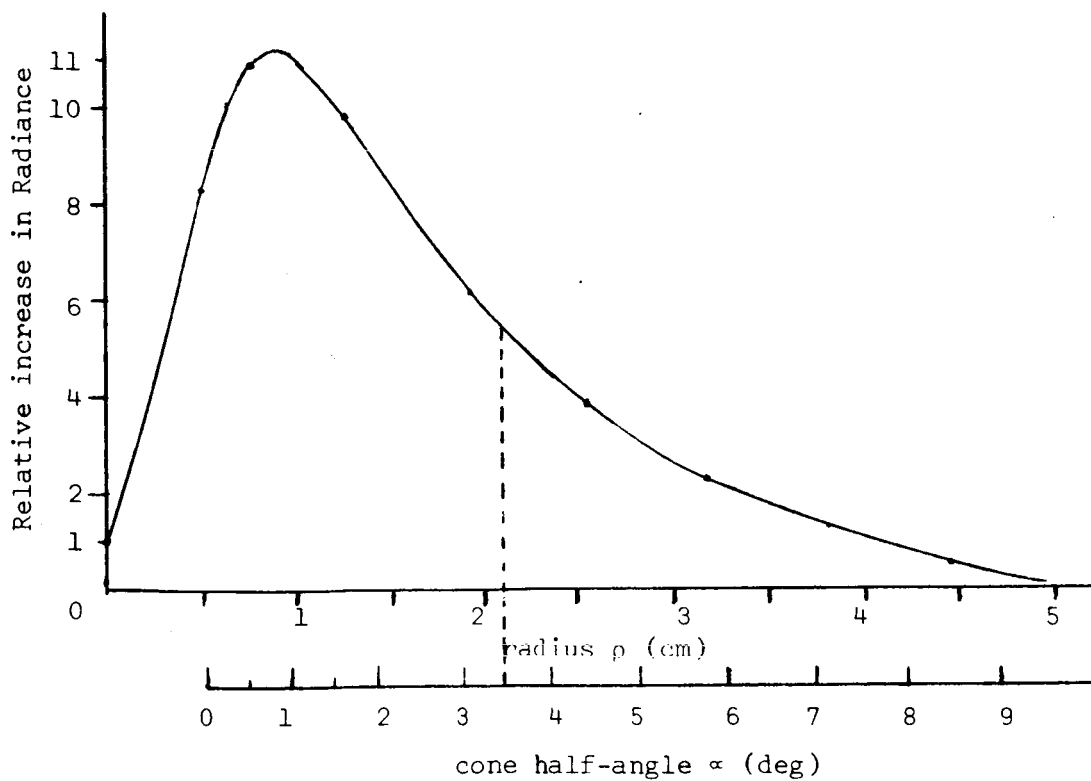


Fig. 11 Relative increase in radiance due to a hot ring of radius  $\rho$  and width 4.0 mm.



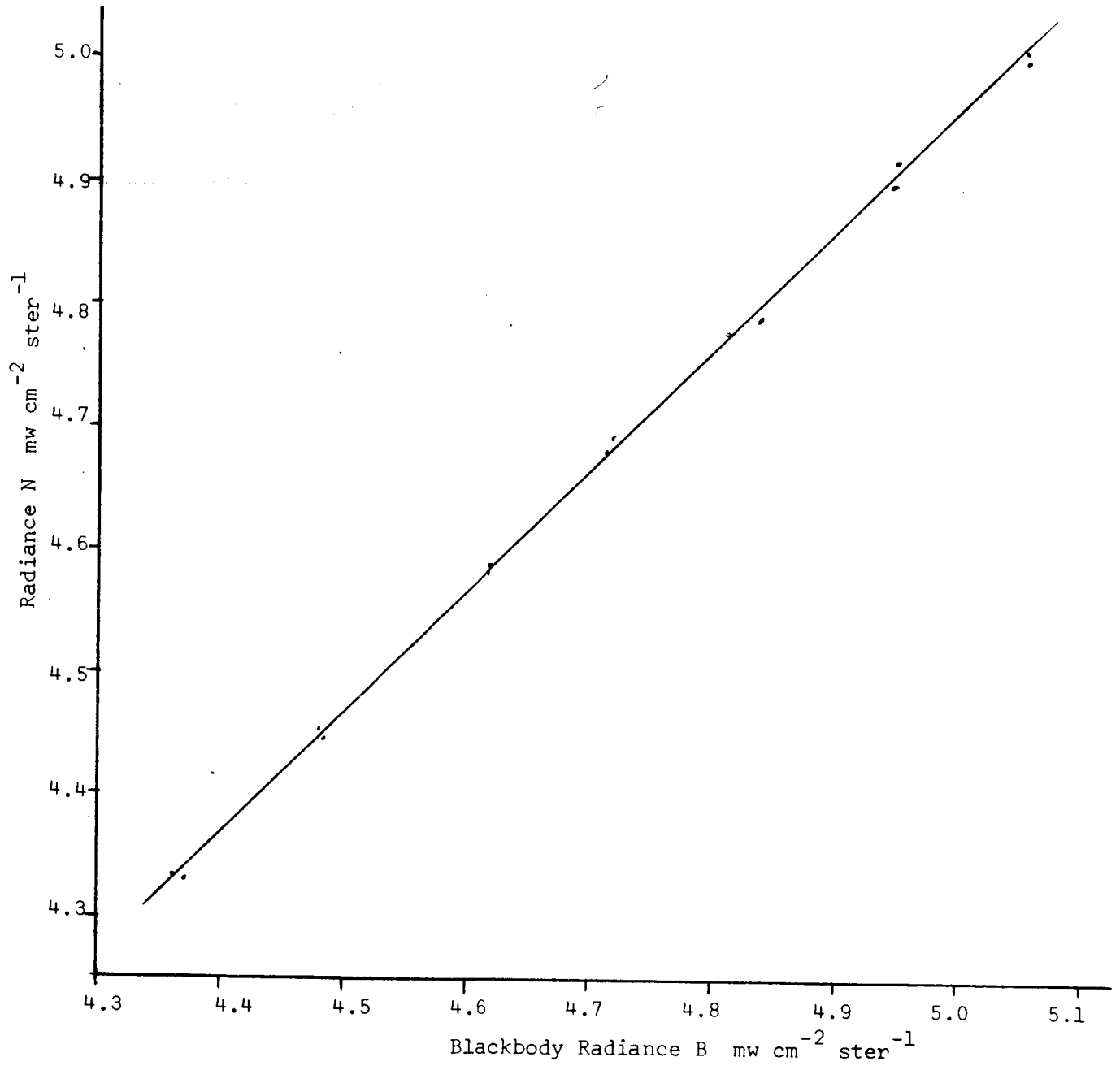


Fig.12 Radiance of Parson's Optical Black Paint as measured in the cold box versus blackbody radiance.

REFERENCES

- Alkezweeny, A.J. and P.V. Hobbs, "The reflection spectrum of ice in the near infrared". J. Geoph. Res., 71, pp. 1083 - 1086, 1966.
- Bandeem, W.R. Experimental Approaches to Remote Atmospheric Probing in the Infrared from Satellites, Goddard Space Flight Center, Greenbelt, Maryland, 50pp., 1968.
- Best, A.C., "The size distribution of raindrops." Quart. J. Roy. Met. Soc., 76, pp. 16-36, 1950.
- Blanchard, D.C., "Raindrop size-distribution in Hawaiian rains." J. Met., 10, pp. 457-473, 1953.
- Buettner, K.J.K., R. Dana, K. Katsaros and W. Kreiss, "On the use of intermediate infrared and microwave infrared in weather satellites." Third Annual Report, Contract NsG-632, N.A.S.A., Goddard Space Flight Center, Greenbelt, Maryland, 1967.
- Catow, C., W. Nordberg, P. Thaddeus, and G. Ling, "Preliminary results from aircraft flight tests of an electrically scanning microwave radiometer." Tech. Rept. X-662-67-352, Goddard Space Flight Center, Greenbelt, Maryland, 1967.
- Conaway, Jack and C.H.M. Van Bavel, "Evaporation from a wet soil surface calculated from radiometrically determined surface temperatures." Journal of Applied Meteorology, V. 6, No. 4, pp. 650 - 655, August, 1967.
- Conaway, Jack and C.H.M. Van Bavel, "Remote measurement of surface temperature and its application to energy balance and evaporation studies of bare soil surfaces." Interim Report, Tech. Report Ecom 2-67P-1, Dec., 1966.
- Cox, Charles, and Munk, Walter, "Measurement of the roughness of the sea surface from photographs of the sun's glitter." J. of the Optical Society of America, 44, p. 838, 1954.
- Defant, A., Physical Oceanography, Pergamon Press, New York, p. 57, 1961.
- Gunn, R., and G.D. Kinzer, "The terminal velocity of fall for water droplets in stagnant air." J. Met., 6, pp. 243-248, 1949.
- Hazelworth, John B., "Water temperature variations resulting from hurricanes." Am. Geoph. Un., 49, p. 204, 1968.

- IGY Instruction Manual, Part VI, "Radiation Instruments and Measurements." Annals of IGY V. 5, 436, 1958.
- Janza F.J. A Comparison of the Microwave Scatterometer and Radiometer For Sea-State Measurements. Ryan Electronics and Space Systems, San Diego, California, 1968.
- Kerr, Donald E. Propagation of Short Radio Waves, Dover, New York, 1965.
- McFadden, James D., "Sea surface temperature and hurricane movement." Transactions Am. Geoph. Un., 49, p.203, 1968.
- Ramsey, W.Y., "Specular reflectance of paints from 0.4 to 40.0 microns." Report No. 31, Meteorological Satellite Laboratory, U.S. Dept. of Commerce, April, 1964.
- Timmermans, J. The Physico - Chemical Constants of Binary Systems in Concentrated Solutions. Vol. 3, p. 332, New York, 1956-1960.
- Yost and S. Wenderoth, "Multispectral color aerial photography." J. Amer. Soc. Photogrammetry, 33, pp. 1020-1033, 1967.